



**HAL**  
open science

## Non linear dynamical behaviour of shape memory alloys and optimisation of damping effect. Study of a passive damper

Frédéric Thiebaud, Manuel Collet, Emmanuel Foltete, Christian LExcellent,  
Vincent Placet

### ► To cite this version:

Frédéric Thiebaud, Manuel Collet, Emmanuel Foltete, Christian LExcellent, Vincent Placet. Non linear dynamical behaviour of shape memory alloys and optimisation of damping effect. Study of a passive damper. 10th European Mechanics of Materials Conference "Multi-phases and multi-components materials under dynamic loading" (EMMC-10), Jun 2007, Kazimierz Dolny, Poland. pp.338-342. hal-00348449

**HAL Id: hal-00348449**

**<https://hal.science/hal-00348449>**

Submitted on 27 Apr 2023

**HAL** is a multi-disciplinary open access archive for the deposit and dissemination of scientific research documents, whether they are published or not. The documents may come from teaching and research institutions in France or abroad, or from public or private research centers.

L'archive ouverte pluridisciplinaire **HAL**, est destinée au dépôt et à la diffusion de documents scientifiques de niveau recherche, publiés ou non, émanant des établissements d'enseignement et de recherche français ou étrangers, des laboratoires publics ou privés.



Distributed under a Creative Commons Attribution 4.0 International License

## NONLINEAR DYNAMICAL BEHAVIOR OF SHAPE MEMORY ALLOYS AND OPTIMIZATION OF THE DAMPING EFFECT

F. THIEBAUD\*, M. COLLET\*, E. FOLTÊTE\*, C. LEXCELLENT\*, V. PLACET\*

\*Institut Femto-ST / dpt. Laboratoire de Mécanique Appliquée, 25000 Besançon, France

*e-mail:* [frederic.thiebaud2@univ-fcomte.fr](mailto:frederic.thiebaud2@univ-fcomte.fr)

**Abstract:** Shape Memory Alloys (SMAs) are good candidates for being used as passive dampers, strain sensors, stiffness or shape drivers. In order to develop the use of these alloys in structural vibration control, we present in this paper how the implementation (Thiebaud & al. (2007)) of a phenomenological model based on the  $R_l$  model (Raniecki & al. (1992)) in a finite element code is used. This implementation permits us to simulate internal loops in order to characterize the stiffness and the damping effect by an Equivalent Complex Young's Modulus approach under many static strain offsets. The results confirmed a dynamic mechanical analysis led on a SMA wire sample and, clearly show us the influence of an initial static strain offset and the amplitude of vibration on the damping effect and the stiffness.

**Keywords:** Shape Memory Alloys – Numerical Implementation – Equivalent Complex Young's Modulus – Damping Effect – DMA Analysis – Harmonic Balance

### 1. Introduction

Shape Memory Alloys (SMAs) are widely studied as smart materials because of its potentiality to be used as dampers, absorbers or actuator elements. For damping applications, the understanding of the material dynamic behavior is needed. One uses the loss of stiffness linked to the martensite transformation between a mother phase called austenite and a product phase called martensite. Also the process of reorientation of martensite platelets called sometimes pseudoplasticity can be used. In this case, the SMAs elements are used as absorbers mainly for seismic applications (Bono & al. (1999), Tirelli & al. (2000), Magonette & al. (2000)). The best example of structure control by SMAs can be founded in the basilic *S'* François d'Assise in Italy. For technological applications, the effect of a static strain offset on the dynamical response of a system is investigated. In order to evaluate stiffness and damping evolutions during the martensite transformation, a method based on an Equivalent Complex Young's Modulus determination (Collet & al. (2001)) is initiated. In this present paper at first, a phenomenological model at the macroscopic scale in the frame of the thermodynamics of irreversible process devoted to multiaxial pseudoelasticity is recalled. Taking into account that experiments are investigated on a SMA wire (one dimension), only a one-dimensional version of the so-called  $R_l$  model (Raniecki & al. (1992)) is written. In a second stage, Equivalent Complex Young's Modulus method is quickly described, a dynamic mechanical analysis led on SMAs wires samples is led. Finally the stiffness and damping evolution as the function of the loading path investigated and comparison between simulations and experiments, exposed.

### 2. A thermomechanic model for the pseudoelasticity

Modeling material behavior needs classically a choice of a thermodynamic potential and also a dissipation potential function or some yield functions of phase transformation (as it is the

scheme in plasticity). Hence, a Helmholtz free energy and two yield functions, the first for the forward transformation ( $A \rightarrow M$ ) and the second for the reverse phase transformation ( $M \rightarrow A$ ) are chosen. The appropriate internal variable is the volume fraction of martensite  $M$ :  $\xi$  ( $(1-\xi)$  being the volume fraction of austenite  $A$ ).

The free energy function of the two phases REV (Reference Elementary volume) is chosen as:

$$\Phi(\varepsilon, T, \xi) = \frac{1}{2} \frac{E}{\rho} (\varepsilon - \gamma\xi - \alpha_0(T - T_0))^2 + u_0^1 - Ts_0^1 - \xi\pi_0^f(T) + \xi(1-\xi)\phi_{ii}(T) \quad (2.1)$$

where  $\pi_0^f(T)$  represents the thermodynamic force associated to the phase transformation under the stress free state:

$$\pi_0^f(T) = \Delta u^* - T\Delta s^* \quad (2.2)$$

with  $\Delta u^*$  ( $\Delta s^*$ ) the difference between internal energy (entropy) of austenite and martensite defined by:

$$\Delta u^* = u_0^{*1} - u_0^{*2}, \quad \Delta s^* = s_0^{*1} - s_0^{*2}. \quad (2.3)$$

$\phi_{ii}$  represents the coefficient of internal interaction between the martensite platelets and the mother phase:

$$\phi_{ii}(T) = \bar{u}_0 - T\bar{s}_0. \quad (2.4)$$

In a classical way, the stress can be obtained as:

$$\sigma = \rho \frac{\partial \phi}{\partial \varepsilon} = E(\varepsilon - \gamma\xi - \alpha_0(T - T_0)). \quad (2.5)$$

The thermodynamic force associated to the progress of the phase transformation can be written as:

$$\pi_f(\sigma, \xi, T) = -\frac{\partial \phi}{\partial \xi} = \frac{\gamma\sigma}{\rho} + \pi_0^f(T) - (1-2\xi)\phi_{ii}(T). \quad (2.6)$$

A classical calculation delivers the expression of the increment of dissipation  $dD$  which cannot be negative:

$$dD = \pi_f d\xi \geq 0. \quad (2.7)$$

Thus, the present inequality precludes the forward phase transformation if  $\pi^f \geq 0$  and the reverse one if  $\pi^f \leq 0$ . One has to note that  $\pi^f = 0$  implies the equilibrium condition. In order to specify the kinetic equations driving the phase transformation, we presume that there exist two functions  $\psi^\alpha(\pi^f, \xi)$ , ( $\alpha=1,2$ ) such that an active process of parent phase decomposition can only proceed when  $d\psi^1 = 0$  and an active process of martensite decomposition can only proceed if  $d\psi^2 = 0$ . These yield functions are chosen as:

$$\psi^1 = \pi_f - k^{(1)}(\xi), \quad \psi^2 = -\pi_f + k^{(2)}(\xi). \quad (2.8)$$

The expression of  $k^\alpha(\xi)$  are built to give kinetics in agreement with the measurements of metallurgists as Koistinen and Marburger (Koistinen & al. (1959)):

$$k^{(1)}(\xi) = -A_1 \ln(1-\xi), \quad k^{(2)}(\xi) = A_2 \ln(\xi). \quad (2.9)$$

Thanks to derivation, the kinetic laws for forward and reverse phase transformation are obtained:

$$\xi_{A \rightarrow M}(\dot{\sigma}, \dot{T}, \xi) = \frac{\frac{\gamma\dot{\sigma}}{\rho} - \Delta s^* \dot{T}}{\frac{A_1}{1-\xi} - 2\phi_{ii}(T)}, \quad \xi_{M \rightarrow A}(\dot{\sigma}, \dot{T}, \xi) = \frac{\frac{\gamma\dot{\sigma}}{\rho} - \Delta s^* \dot{T}}{\frac{A_2}{\xi} - 2\phi_{ii}(T)}. \quad (2.10)$$

It is known that the forward transformation is exothermic and the reverse transformation endothermic. Many studies have shown or just taken into account the temperature influence: for dynamic loadings by Collet (Collet & al. (2001)) or for the rate effects loading by LExcellent and Rejzner (LExcellent & al. (2001)). The phase transformation which occurs during a period of vibration is supposed to be adiabatic. In this case, the expression of the heat equation is thus obtained:

$$Cv \cdot \dot{T} = (\pi_f(\sigma, T, \xi) + T \cdot \Delta s^*) \dot{\xi}. \quad (2.11)$$

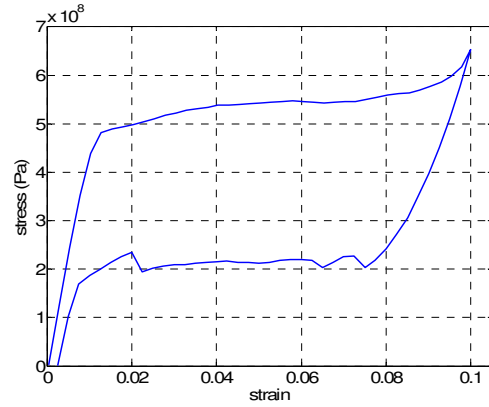
This equation is used to quantify the temperature evolution inside the SMA wire sample.

### 3. Prediction of the dynamical behavior

This study will allow us to characterize the stiffness and damping of SMAs as function of a static strain offset  $\varepsilon_0$  and the amplitude of vibration  $\varepsilon_m$  by using the Equivalent Complex Young's Modulus approach. First of all, a simple strain load/unload until 10% is done on a NiTi wire (length:  $L_0=30\text{mm}$  and diameter:  $D=0.59\text{mm}$ ) in order to identify the constants of the used SMA (NiTi). The following figure 1 shows us the tensile testing machine with the NiTi wire (a) and, the SMA wire response (b).



a. Tensile testing machine with the NiTi wire



b. SMA wire response

Figure 1. Tensile test for the identification of the constants of the NiTi wire

Thus, the used constants are identified and recalled in the table 1.

Table 1. Constants used for NiTi alloy

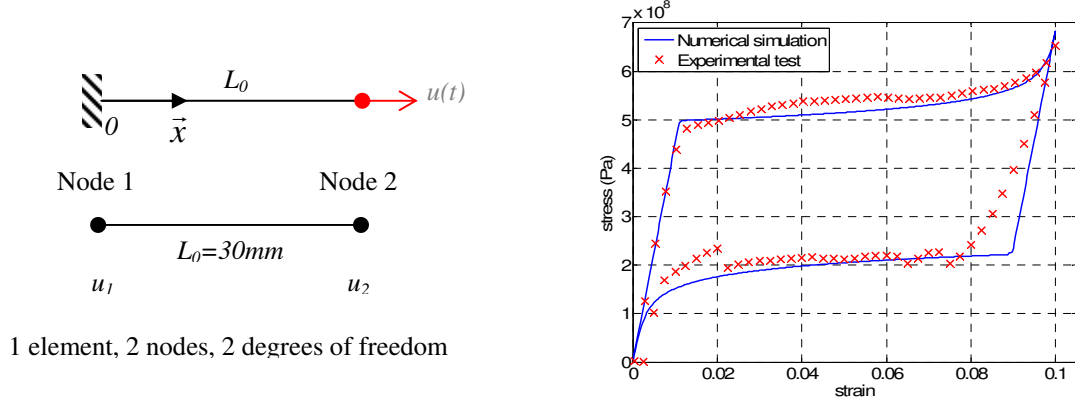
Designation	Notation	Value	Unit
<b>Mechanical</b>			
Young's modulus	$E$	52	GPa
Transformation strain	$\gamma$	8.5%	$\emptyset$
<b>Physical</b>			
External temperature	$T_0$	293	K
Density	$\rho$	6723	kg/m <sup>3</sup>
Driving force	$\pi_0^f(T_0)$	-4538	J/kg
Coefficient of internal interaction	$\phi_{it}(T_0)$	1782	J/kg
Coefficient A1	$A_1$	699	J/kg
Coefficient A2	$A_2$	280	J/kg

#### 3.1 Numerical implementation

Taking into account the pseudoelastic behavior explained in the section 2, the equilibrium of a wire cross-section leads us to the vibration wave equation of the wire in tension:

$$\rho \frac{\partial^2 u(x,t)}{\partial t^2} = E \frac{\partial^2 u(x,t)}{\partial x^2} - \gamma E \frac{\partial \xi}{\partial x}. \quad (3.1)$$

This equation is thus coupled with both kinetic equations and the heat equation: only one linear Lagrange element is used to build the finite element model (Thiebaud & al. (2007)). This model is illustrated on the figure 2a and a simulated cycle on the figure 2b. One can notice a good correspondence between the numerical simulated cycle and the tensile test of the sample.



a. FEM model with Lagrange element

b. Tensile testing machine with the NiTi wire

Figure 2. Numerical implementation of the wire in tension

### 3.2 Equivalent Complex Young's Modulus

The Equivalent Complex Young's Modulus is a powerful tool usually used to describe the elastic behavior and the damping properties of a viscoelastic material under dynamical loading (Collet (2001)). This modulus can be generalized to quantify, on the first harmonic, the response of a nonlinear hysteretic material.

The constitutive relation between the stress  $\sigma$  and strain  $\varepsilon$  for a dissipative material subject to steady state harmonic can be written as:

$$\sigma = E^* \varepsilon = E(1 + i\eta) \varepsilon \quad (3.2)$$

where  $E^*$  is the complex modulus,  $E$  the storage modulus and  $\eta$  the loss factor. For a harmonic strain input  $\varepsilon(t) = \varepsilon_0 + \varepsilon_m \cos(\omega t)$  and the corresponding measured stress  $\sigma(t)$ , the storage modulus and the loss factor are evaluated as :

$$E = \frac{\omega}{2\pi\varepsilon_0^2 + \pi\varepsilon_m^2} \left\{ \varepsilon_0 \int_0^T \sigma(t) dt + \varepsilon_m \int_0^T \sigma(t) \cos \omega t dt \right\} \quad (3.3)$$

$$E\eta = -\frac{\omega}{\pi\varepsilon_m} \int_0^T \sigma(t) \sin \omega t dt. \quad (3.4)$$

Thus, the harmonic strain input  $\varepsilon(t)$  and the corresponding stress  $\sigma(t)$  are evaluated as:

$$\varepsilon(t) = \text{Re}\{\hat{\varepsilon}(t)\} = \varepsilon_m \cos(\omega t) \quad (3.5)$$

$$\sigma(t) = \text{Re}\{\hat{\sigma}(t)\} = E\varepsilon_m (\cos(\omega t) - \eta \sin(\omega t)). \quad (3.6)$$

A graphical representation of both previous equations in the  $(\varepsilon, \sigma)$  axis system yields the classical stress/strain elliptical hysteresis cycle of a damping material subjected to harmonic excitations of amplitude  $\varepsilon_m$ , figure 3.

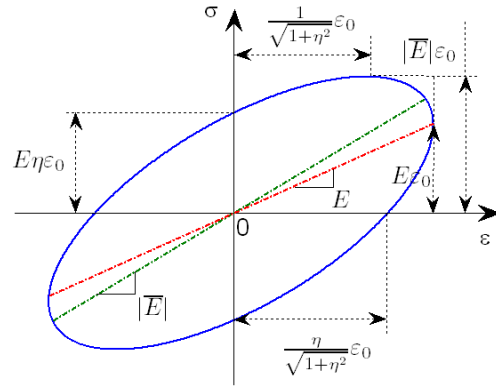


Figure 3. Hysteresis cycle of a dissipative material with storage factor and loss modulus undergoing cyclic strain oscillations of amplitude  $\varepsilon_0$ .

### 3.3 Experimental investigations

In order to predict the dynamical behavior of SMAs, a series of experimental tests is led on the tensile testing machine. This dynamic mechanical analysis is automatically done by the machine software, with a FFT Fourier analysis. The static strain offset  $\varepsilon_0$  (and thus  $u_0$ ) is reached linearly and ten vibration cycles are simulated with amplitude of  $\varepsilon_m$  (and thus  $u_m$ ) and a frequency of 1Hz in order to get a stabilize response cycle. Finally, only this last stabilized response is kept and used to evaluate the storage modulus and the loss factor by the resolution of both equations (3.5) and (3.6). A suitable value of  $\varepsilon_0$  is fixed at 4%. Beyond this limit, the fatigue effects can be sufficient to quickly lead the wire to the rupture. Also,  $\varepsilon_m$  is with most equal to  $\varepsilon_0$ . The figure 4 shows us the command function (a) and the material answer (b). The table 2 presents the used values for  $U_0$  and  $U_m$ .

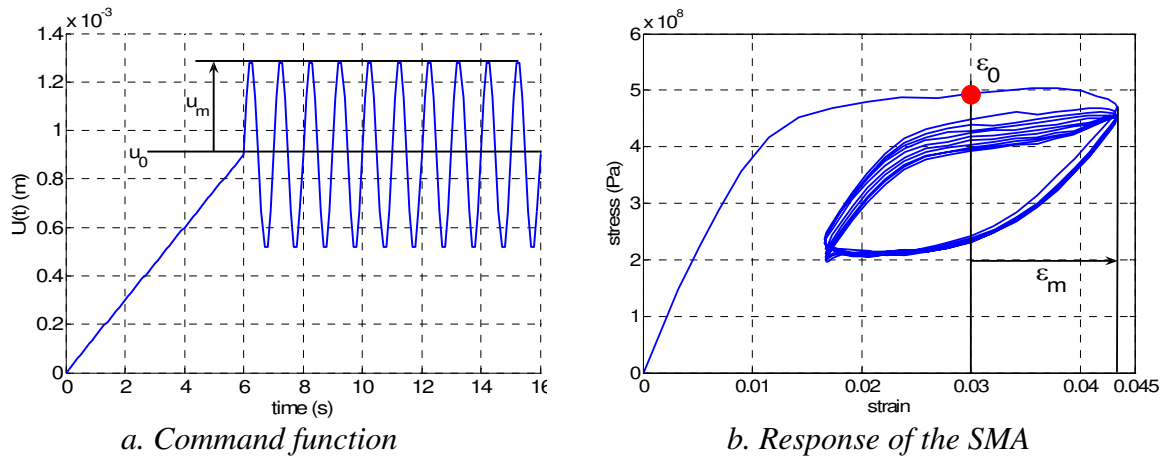


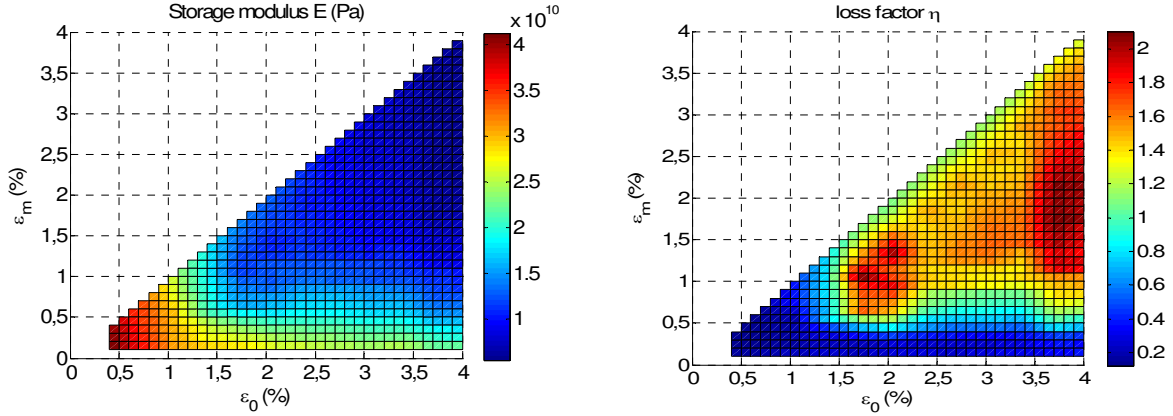
Figure 4. Vibration tests

Table 2. Used values for  $U_0$  and  $U_m$

$U_0$ (mm)	0.1	0.2	0.3	0.4	0.5	0.6	0.7	0.8	0.9	1.0	1.1	1.2
$U_m$ (mm)	0.01	0.01	0.01	0.01	0.01	0.01	0.01	0.01	0.01	0.01	0.01	0.01
	0.02	0.02	0.02	0.02	0.03	0.03	0.03	0.04	0.04	0.04	0.04	0.05
	0.03	0.04	0.03	0.04	0.05	0.06	0.05	0.08	0.09	0.07	0.07	0.07
	0.04	0.06	0.06	0.08	0.10	0.12	0.07	0.16	0.18	0.10	0.11	0.12
	0.05	0.08	0.09	0.12	0.15	0.18	0.14	0.24	0.27	0.20	0.22	0.24
...	...	...	...	...	...	...	...	...	...	...	...	...

	0.09	0.18	0.27	0.36	0.45	0.54	0.63	0.72	0.81	0.90	0.99	1.08
	0.10	0.20	0.30	0.40	0.50	0.60	0.70	0.80	0.90	1.00	1.10	1.20

Finally, one can represent on the figure 5, the measured storage modulus  $E$  and the measured loss factor  $\eta$  in function of the static strain offset  $\varepsilon_0$  and the amplitude of vibration  $\varepsilon_m$ .

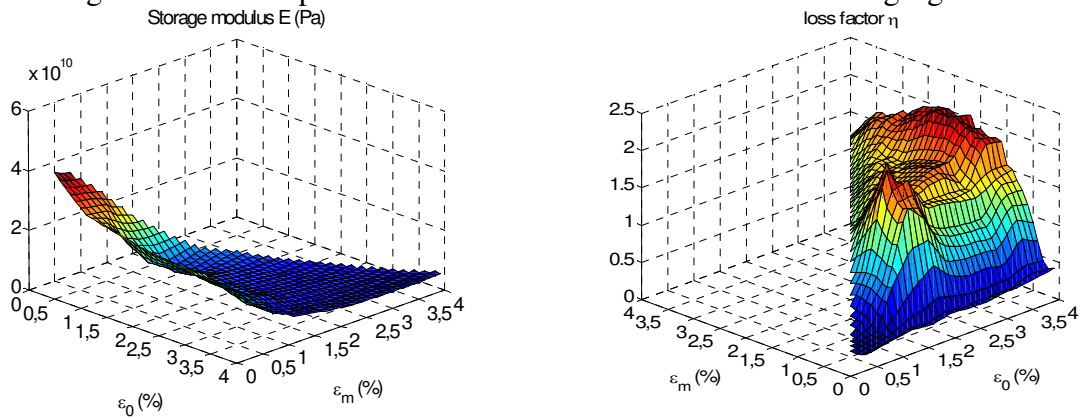


a. Measured storage modulus  $E$

b. Measured loss factor  $\eta$

Figure 5. Equivalent Complex Young's Modulus measured components in function of the static strain offset  $\varepsilon_0$  and the amplitude of vibrations  $\varepsilon_m$ .

The same figures are now represented in three dimensions on the following figure 6:



a. Measured storage factor  $E$

b. Measured Loss factor  $\eta$

Figure 6. Equivalent Complex Young's Modulus measured components in function of the static strain offset  $\varepsilon_0$  and the amplitude of vibration  $\varepsilon_m$  - representation in three dimensions

The following observations can be made based on these experiments: as the excitation amplitude increases, a decrease of the storage modulus is observed. This storage modulus is minimal for a static strain offset between 1.25% to 4% which corresponds to a strain located on the plateau of transformation. As the excitation increases, an increase of the loss factor is observed. This loss factor is maximal for a static strain offset between 1.5% to 4% which corresponds to a deformation located on the plateau of transformation too. A priori, one can conclude that the wire must be partially transformed to present interesting damping properties.

### 3.4 Simulations, numerical results

In order to confront these previous results given in the section 3.3, a series of numerical tests is done. The storage factor  $E$  and the loss modulus  $\eta$  are thus calculated in Matlab<sup>®</sup> as post

processing with the same values of  $U_0$  and  $U_m$  exposed in the table 2. Thus, one can represent on the figure 7, the storage modulus  $E$  (7a) and the loss factor  $\eta$  (7b) versus the static strain offset  $\varepsilon_0$  and the vibration strain  $\varepsilon_m$ .

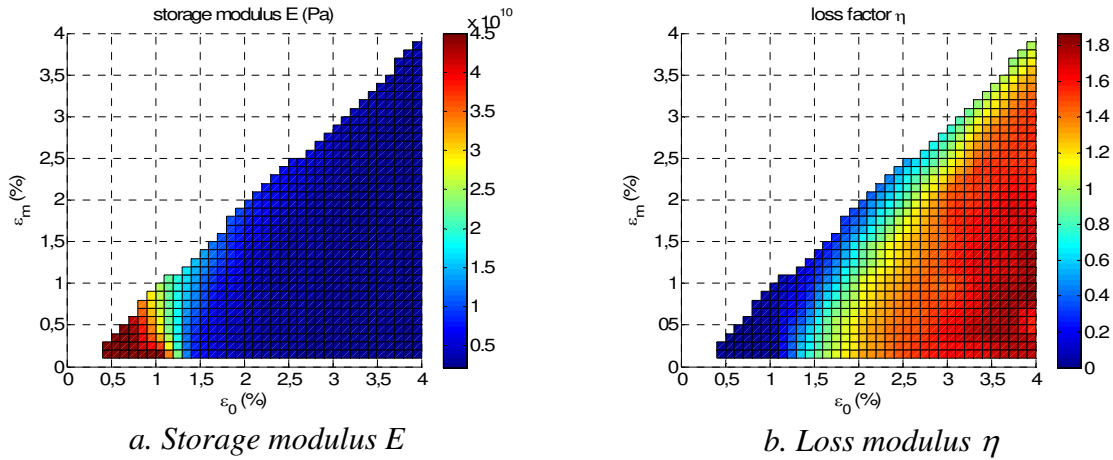


Figure 7. Equivalent Complex Young's Modulus components in function of the static strain offset  $\varepsilon_0$  and the amplitude  $\varepsilon_m$ .

The same figures are now represented in three dimensions on the following figure 8:

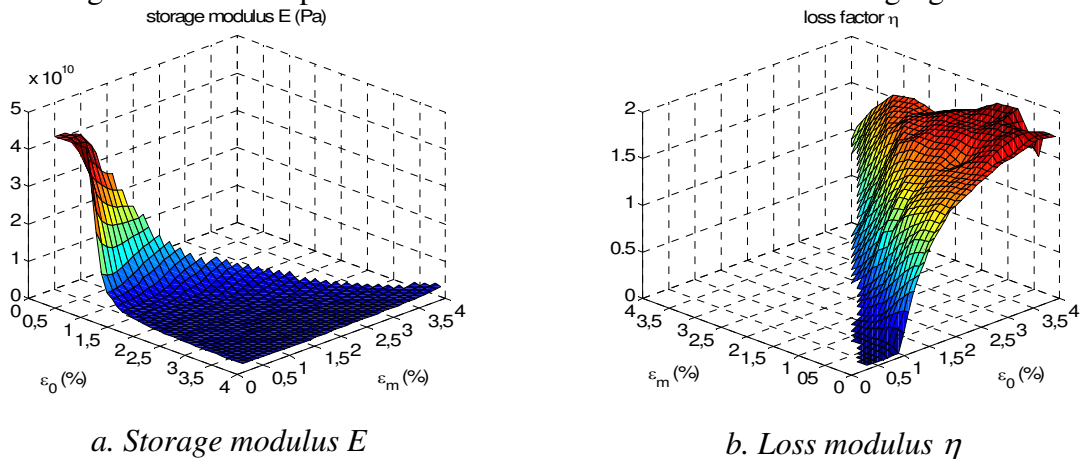


Figure 8. Equivalent Complex Young's Modulus components in function of the static strain offset  $\varepsilon_0$  and the amplitude  $\varepsilon_m$  - representation in three dimensions

The following observations can be made based on the results: as the excitation amplitude increases, an decrease of the storage modulus is observed. This storage modulus is minimal for a static strain offset between 1.5% to 4% which corresponds to a deformation located on the plateau of transformation. As the excitation increases, a increase of the loss factor is observed. This loss factor is maximal for a static strain offset between 1.5% to 4% which corresponds to a deformation located on the plateau of transformation too. But a difference is noticed for a static strain offset upper than 1.5% and small amplitude of vibration: whereas the experiments predict that the damping capacity is negligible, the computation shows a high damping capacity inside this area. Everywhere else, the numerical simulations are in good agreement with the experiments leaded on the tensile testing machine.

## Conclusion

In this paper, the characterization of the dynamic behavior of Shape Memory Alloys versus of two parameters: the amplitude of vibration and the static strain offset, has been done by using

the Equivalent Complex Young's Modulus approach. In a first part, the use of the implementation of a phenomenological model has been recalled in order to simulate internal loops for many cases of displacement loadings. Those internal loops were necessary to use this method. In the second part, the Equivalent Complex Young's Modulus has been presented and the material parameters identified. Many cases of displacement loadings with different values of the static strain offset and the strain vibration have been simulated. At last, the storage modulus and the loss factor (which defined the Equivalent Complex Young's Modulus) have been calculated from numerical simulations and several cycles done on a testing tensile machine. Thus, this study permits us to highlight the existence of a high damping zone which is localized for static strain offsets between 1.5% and 4%% and small strains vibration (the totally pseudoelastic behavior zone of the SMA). These investigations permit us to improve the nonlinear modeling of SMAs in order to develop and optimize applications for the control and the damping in civil engineering.

### References

- Bono F. Tirelli D.,1999, Characterisation of materials for the innovative antisismic techniques. *Internal reports, ELSA Laboratory.*
- Collet M. Foltête E. Lexcellent C.,2001, Analysis of the behavior of a shape memory alloy beam under dynamical loading. *Eur. J.Mech. A/Solids*, 20, 615-630.
- Lexcellent C. Rejzner J.,1998, Modeling of the strain rate effect, creep and relaxation of a NiTi Shape Memory Alloy under tension (compression)-torsional proportional loading in the pseudoelastic range. *Smart Mater. Struct.*9,613-621.
- Marburger R.E. Koistinen D.P.,1959, A general equation prescribing the extent of the austenite-martensite transformation in pure non-carbon alloys and plain carbon steels. *Acta Met.* 7,55-69.
- Molina J. Renda V. Magonette G. Marazzi F.,2000, Structural control : Experimental activity at elsa. *Internal report, ELSA Laboratory.*
- Raniecki B. Lexcellent C. Tanaka K.,1992, Thermodynamic models of pseudoelastic behavior of Shape Memory Alloys, *Arch. Mech.*,44(3),261-284.
- Thiebaud F. Collet M. Foltête E. Lexcellent C., 2007, Implementation of a multi-axial pseudoelastic model to predict the dynamic behavior of Shape Memory Alloys, *Smart Material and structure.*
- Tirelli D. Renda V. Bono F.,2000, Characterisation of shape memory alloys applications to the retrofitting of brick masonry wall by the pseudo-dynamic method and numerical models. *Internal report, ELSA Laboratory.*